

## An in-plane, bi-directional electrothermal MEMS actuator

This article has been downloaded from IOPscience. Please scroll down to see the full text article.

2006 J. Micromech. Microeng. 16 2067

(<http://iopscience.iop.org/0960-1317/16/10/020>)

View [the table of contents for this issue](#), or go to the [journal homepage](#) for more

### Download details:

IP Address: 128.100.48.236

The article was downloaded on 08/10/2010 at 15:54

Please note that [terms and conditions apply](#).

# An in-plane, bi-directional electrothermal MEMS actuator

Roberto Venditti<sup>1</sup>, Jacky S H Lee<sup>1</sup>, Yu Sun<sup>1</sup> and Dongqing Li<sup>2</sup>

<sup>1</sup> Advanced Micro and Nanosystems Laboratory, Department of Mechanical and Industrial Engineering, University of Toronto, Toronto, ON M5S 3G8, Canada

<sup>2</sup> Department of Mechanical Engineering, Vanderbilt University, Nashville, TN 37235, USA

E-mail: [sun@mie.utoronto.ca](mailto:sun@mie.utoronto.ca)

Received 21 May 2006, in final form 25 July 2006

Published 29 August 2006

Online at [stacks.iop.org/JMM/16/2067](http://stacks.iop.org/JMM/16/2067)

## Abstract

This paper presents the design and testing results of an electrothermally driven MEMS (microelectromechanical systems) actuator. Different from conventional uni-directional U-beam thermal actuators, this in-plane bi-directional electrothermal (IBET) actuator is capable of producing displacements in two directions as a single device. It is important to note that merely coupling two conventional uni-directional U-beam electrothermal actuators is insufficient to achieve bi-directional motion, as the resistance from the oppositely configured actuator severely limits net motion and leads to poor performance. An optimized IBET design was obtained through numerical simulation using finite element modeling. The devices were fabricated using the standard polyMUMPs surface micromachining process. Experimental results demonstrate that the IBET microactuators have a displacement range of 12  $\mu\text{m}$  (6  $\mu\text{m}$  in either direction).

(Some figures in this article are in colour only in the electronic version)

## Introduction

MEMS microactuators are important devices for producing motion at the micro and nanometer scales. Among commonly used actuation mechanisms (electrostatic, piezoelectric and electrothermal), electrothermal microactuation features high force output and the ease-to-implement using conventional microfabrication processes [1]. Despite these advantages, electrothermally driven devices are limited in response time. Since the response of a thermal actuator relies on heat-transfer rates, it unavoidably exhibits slower operating characteristics than other types of microactuators. Electrothermal microactuators typically can be driven at frequencies up to 1 kHz [2]. In contrast, piezoelectric microactuators are capable of operating on the order of 100 kHz [3] and electrostatic microactuators up to GHz [4]. Thus, electrothermal microactuators are usually employed in high-force, low-frequency applications.

Electrothermal actuation relies on thermal expansion caused by non-uniform Joule heating. In order to achieve motion, device components must thermally expand to a different extent, causing the device to warp or deform. Besides the more recent development of V-beam electrothermal

microactuators [5] that will not be discussed in this paper, the electrothermal microactuators used most often are of the U-beam type [6]. These devices were first demonstrated by Guckel in 1992 and since then have found a wide range of applications in microsystem design [2, 7, 8]. As illustrated schematically in figure 1(a), when a current is passed through the anchors, the 'hot' arm is heated much more than the 'cold' arm due to a higher current density, resulting in more Joule heating. The 'hot' arm expands and causes the device to bend downwards. The key geometric parameters of such a U-beam electrothermal actuator are the length of the flexure (the thinner beam connecting the 'cold' arm to the anchor) and the length of the 'hot' arm. If the flexure is made too short, the device becomes stiff and thus, more difficult to deflect. Optimization must be conducted to determine the optimal flexure length. It is well understood that a longer 'hot' arm can produce a larger deflection; however, this also produces a higher chance of failure such as due to stiction in surface micromachined actuators [10].

Conventional U-beam electrothermal microactuators are only capable of producing deflections along a single direction. Moulton [7] proposed that if a conventional U-beam actuator were electrically connected in parallel instead of in series,

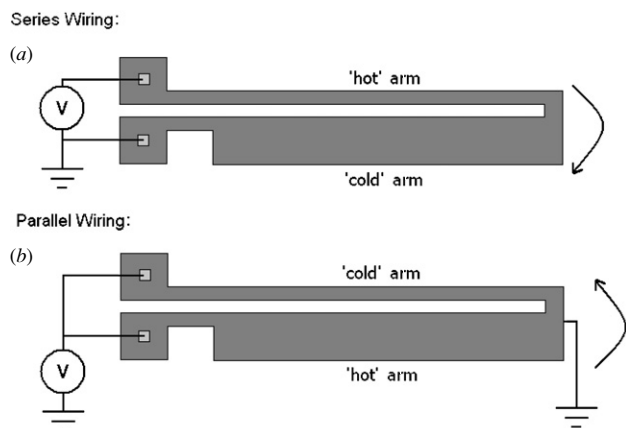


**Figure 1.** Schematic diagram of a basic electrothermal actuator. (a) Series wiring: applied voltage generates a high temperature in the thin arm due to resistive Joule heating, which causes its length to increase. This length change forces a net motion downward. (b) Parallel wiring: applied voltage generates a high temperature in the thick arm due to a higher current draw than the thinner arm which results in a net upward motion.

upward bending motion can be achieved (figure 1(b)). In this configuration, the thicker arm will draw more current than the higher resistance thin arm, and hence will reach a higher temperature due to Joule heating. As such, the thick arm is the ‘hot’ arm, and the net deflection is upward. Unfortunately, this still only represents one-directional motion as the parallel arrangement does not allow for downward bending motion. In theory, a device incorporating both parallel and series wiring arrangements would be able to achieve bi-directional motion. However, the practical limitation is the difficulty of incorporating an electrical connection at the tip of the actuator, thereby rendering a parallel wiring arrangement difficult.

When multiple uni-directional U-beam microactuators are used to achieve bi-directional in-plane motion, the devices must be oriented such that they deflect opposite to one another. Ultimately this actuation scheme results in poor deflection performance. Because forward and reverse devices are permanently attached at all times, any microactuators not being used to produce motion represent a mechanical resistance and resist deflection. Numerical simulations demonstrate that this resistance is extremely high and prevents any significant motion from occurring. This paper reports on the development of electrothermal microactuators with bi-directional functionality as a single integrated device that is less bulky and capable of producing a motion range comparable to conventional U-beam actuators. An optimized design of an in-plane bi-directional electrothermal (IBET) microactuator is presented including design analysis and experimental results obtained from surface microfabricated devices. It needs to be noted that several out-of-plane bi-directional electrothermal actuators were previously demonstrated [9]. To the best knowledge of the authors, no electrothermal microactuators as a single integrated device have yet been demonstrated that are capable of producing in-plane, bi-directional motion.

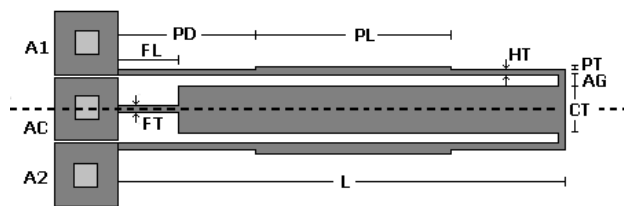


**Figure 2.** Schematic diagram of an IBET actuator. The device moves downwards when voltage is applied at A1, and both AC and A2 are grounded. Upward motion results from applied voltage at A2 and ground at A1 and AC. Labels correspond to dimensions given in table 2.

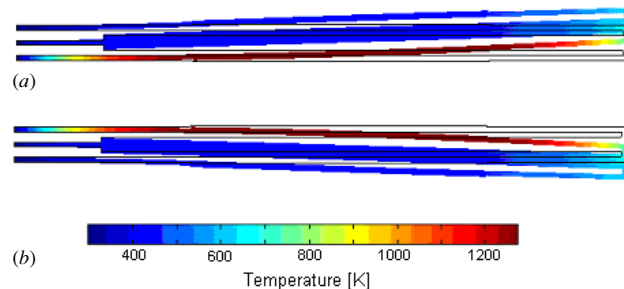


**Figure 3.** Simulated displacement under an applied input power of 51 mW. (a) Upward bending motion. (b) Downward bending motion.

### Design of IBET microactuators

As shown in figure 2, the IBET microactuator is symmetrically designed, allowing equal in-plane displacements along two directions. In order to make the complete structure bend downwards, A1 is supplied with an input voltage or current, while A2 and AC are grounded. In this configuration, the top ‘hot’ arm has a higher current density while the middle common arm and the bottom ‘hot’ arm have a lower current density. Because of its lower resistivity, the majority of electrical current travels through the common arm to the anchors. Correspondingly, the bottom ‘hot’ arm exhibits a very low current density which results in low Joule heating. Thus, the device bends downwards. Similarly, due to symmetry, when the connections for A1 and A2 are swapped, the device bends upwards. The ‘hot’ arms are padded, or thickened, in the middle portion to maximize the actuator’s deflection. Figure 3 illustrates the IBET actuator’s motion along two directions, as obtained from finite element simulation using FEMLAB®.

The key factor that limits the performance of an electrothermal microactuator is temperature. It was reported that the temperature of a polysilicon device should be kept under 1273 K (1000 °C) to avoid thermal failure and permanent damage [11]. Thus, design optimization was conducted in this study at an equal maximum allowable temperature that was chosen to be 1000 K (~80% of polysilicon’s failure limit). During finite element simulation, input power was adjusted to maintain the equal maximum temperature throughout the optimization process. Physical and material parameters used in simulations are summarized in table 1.

In electrothermal actuator simulations, the thermal boundary conditions must be properly treated. It has been

**Table 1.** Physical/material parameters used in finite element simulation [10, 12, 13].

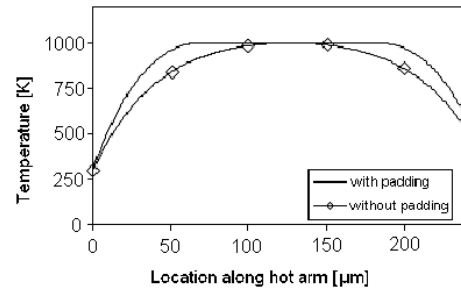
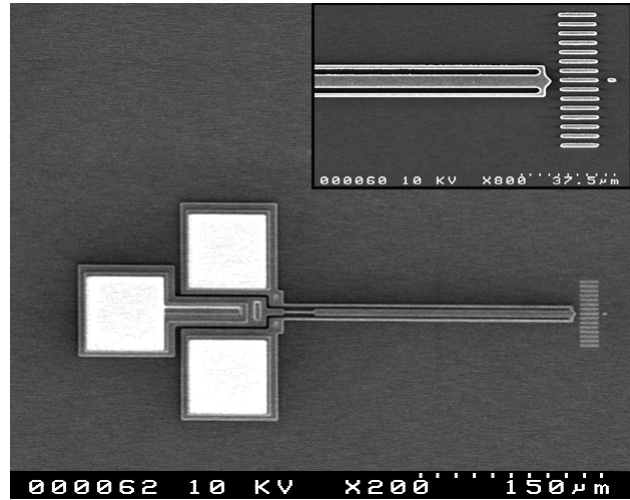
Electrical resistivity of polysilicon	$2.32 \times 10^{-3} \Omega \text{ cm}^{-1}$
Young's modulus	150 GPa
Poisson ratio	0.27
Thermal expansion coefficient	$2.7 \times 10^{-6} \text{ K}^{-1}$
Thermal conductivity of polysilicon	$50 \text{ W m}^{-1} \text{ K}^{-1}$
Thermal conductivity of air	$0.03 \text{ W m}^{-1} \text{ K}^{-1}$

shown that the radiation heat transfer for an electrothermal actuator can be neglected due to its trivial effect on temperature profiles [12]. Convective heat transfer was also considered insignificant and was not included in device simulation. The majority of the heat dissipated in an electrothermal actuator is through heat conduction via the anchors and via air to the substrate. Due to the small separation between the structure and the substrate (e.g.,  $2 \mu\text{m}$ ) in surface micromachined devices, heat conduction between the device and the substrate is significant.

In order to make valid comparisons, the IBET microactuators were designed with similar dimensions of existing U-beam single 'hot'-arm devices. The device length ( $L$  in figure 2) was fixed at  $240 \mu\text{m}$ . Width of the 'hot' arm (HT), flexure (FT) and air gap (AG) were set at  $2 \mu\text{m}$ . Other important design parameters include the length of the flexure (FL), width of the common arm (CT) and sizes of the 'hot'-arm padding (PD-PL-PT). Refer to figure 2 for a labeled illustration of the device, indicating the location of each of the mentioned abbreviated segments ( $L$ , CT, FL, etc).

The common-arm width (CT) is a critical parameter for the IBET actuator because it contributes greatly to the overall mechanical stiffness of the device: the width of the common arm controls the separation distance between the two 'hot' arms and the overall width of the device. This width is the dominant variable for beam stiffness. If CT is too large, the device stiffness is high and the overall deflection is small. In contrast, it is expected that by reducing the width of the common arm the stiffness is lowered and deflection increases. This is true, but with an important limitation. Joule heating in the common arm becomes more significant as its width is reduced. This has the effect of generating an undesirable increase in the thermal expansion of the common arm, which then actually reduces the deflection of the device. Given these considerations, numerical optimization was undertaken to evaluate the device dimensions that would produce a maximum deflection. Optimal conditions were found to exist when the common-arm width (CT) was set at  $6 \mu\text{m}$  and the flexure length (FL) at  $26 \mu\text{m}$ .

The effect of the location and size of the padding (PD-PL-PT) on the 'hot' arms was also investigated. Analytical studies of U-beam electrothermal actuators [12] show that the temperature profile in the 'hot' arm resembles a parabolic shape. This temperature profile is not optimal because only a small region in the 'hot' arm exhibits a high temperature while the rest of the 'hot' arm has a lower temperature. To increase the deflection of an electrothermal actuator under a maximum allowable temperature ( $1000 \text{ K}$  or  $750^\circ\text{C}$ ), a padded region was added to the 'hot' arm in this study. The padded region locally increases the width and volume of the 'hot'

**Figure 4.** Temperature distribution in the IBET actuator hot arm for the two cases with and without padding. Padding helps generate a more uniform distribution profile which improves device performance.**Figure 5.** Scanning electron micrograph of the IBET actuator.**Table 2.** Dimensions of the IBET actuator ( $\mu\text{m}$ ).

HT, FT, AG, L	2, 2, 2, 240
FL, CT	26, 6
PD, PL, PT	70, 115, 0.5

arm. Current density in the padded region is lower than that in the unpadded regions, resulting in reduced Joule heating. Effectively, this padded region flattens the temperature profile (figure 4) creating a greater region of temperature close to the maximum allowable value. Optimization of the padding size under a maximum allowable temperature of  $1000 \text{ K}$  yielded the final device dimensions summarized in table 2.

## Experimental results

An SEM micrograph of an IBET device is shown in figure 5. The IBET microactuators were fabricated using the standard surface micromachining process (polyMUMPs) with a structural layer  $2.0 \mu\text{m}$  thick and  $2.0 \mu\text{m}$  above the substrate. The relationship between deflection and input voltage for the IBET microactuators was characterized. Wire-bonded devices were connected to a power supply and deflections were observed under an optical microscope at  $100\times$  magnification.

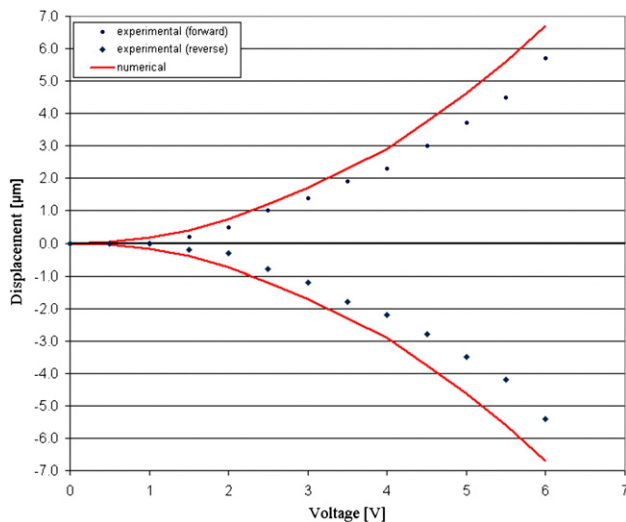


**Figure 6.** Experimental data showing the magnitude of deflection of the IBET actuator as a function of the input voltage. The solid line represents numerical simulation results. Beyond 6 V, permanent deformation occurred due to temperature rise above the working limit of polysilicon.

Voltages were applied in 0.5 V increments, and images of the resultant deflection were recorded via a CCD camera. Experiments proceeded until permanent deformation of the actuators occurred, as evidenced by failure of the device to return to the zero point when no voltage was applied.

Figure 6 shows the deflection response of the IBET device as a function of input voltage. For convenience, the magnitude of deflection is represented in this figure, but it should be noted that negative voltages produced deflection opposite to that of positive voltage (i.e., bi-directional motion). The IBET microactuators were found to have a maximum deflection of approximately  $6 \mu\text{m}$  in either direction, providing a total deflection range of  $12 \mu\text{m}$  that is comparable to existing surface microfabricated U-beam electrothermal actuators [2, 7]. In agreement with finite element simulation, experimental results reveal that the IBET device demonstrates an exponential relationship between displacement and applied voltage. A first reading of figure 6 suggests that the ability of finite element simulation to predict experimental response of IBET actuators deteriorates at higher voltages. In fact, this is not quite true. The value of relative difference between the numerical prediction and experimental result is found to be consistent ( $\sim 0.3$ ) for the voltage range above 2.0 V. Numerical prediction is actually worse at lower voltages, where a relative difference as high as 1.47 is observed (occurring at  $-2.0$  V). A possible explanation for this high relative difference is a hysteresis owing to contact between the beam and the device substrate. This would explain why deflection is not observed until a voltage of 1.5 V is applied (figure 6). Because this phenomenon was not incorporated into the numerical model, it is expected that predictions would differ most in the region where hysteresis is a factor (i.e., at low voltages).

## Conclusions

This paper presented an electrothermally driven MEMS actuator that is capable of producing in-plane deflections along two directions as a single integrated device. An optimal design was obtained through finite element simulation. The devices were fabricated using the standard polyMUMPs surface microfabrication process. In satisfactory agreement with numerical simulation results, testing results demonstrated that the IBET microactuators have a displacement range of  $12 \mu\text{m}$  ( $6 \mu\text{m}$  in either direction).

## Acknowledgments

The authors thank the Canadian Microelectronics Corporation (CMC) for device fabrication support. Financial support from the National Sciences and Engineering Research Council is also acknowledged.

## References

- [1] Krulevitch P, Lee A, Ramsey P, Trevino J, Hamilton J and Northrup M 1996 Thin film shape memory alloy microactuators *J. Microelectromech. Syst.* **5** 270–82
- [2] Comtois J and Bright V 1997 Applications for surface-micromachined polysilicon thermal actuators and arrays *Sensors Actuators A* **58** 19–25
- [3] Roberts D, Li H, Steyn J, Turner K, Mlcak R, Saggere L, Spearing S, Schmidt M and Hagood N 2002 A high-frequency, high-stiffness piezoelectric actuator for microhydraulic applications *Sensors Actuators A* **97–98** 620–31
- [4] Rebeiz G 2003 RF MEMS switches: status of the technology *12th Int. Conf. on Solid State Sensors, Actuators and Microsystems (TRANSDUCERS '03) (Boston, USA, 8–12 June 2003)*
- [5] Que L, Park J-S and Gianchandani Y B 2001 Bent-beam electrothermal actuators—Part I. Single beam and cascaded devices *J. Microelectromech. Syst.* **10** 247–54
- [6] Guckel H, Klein J, Christenson T, Skrobis K, Laudon M and Lovell E 1992 Thermo-magnetic metal flexure actuators *Tech. Dig. Solid-State Sensors and Actuators Workshop (Sacramento, USA, 1992)*
- [7] Moulton T and Ananthasuresh G 2001 Micromechanical devices with embedded electro-thermal-compliant actuation *Sensors Actuators A* **90** 38–48
- [8] Chiou J and Lin W 2004 Variable optical attenuator using a thermal actuator array with dual shutters *Opt. Commun.* **237** 341–50
- [9] Chen W, Chu C, Hsieh J and Fang W 2003 A reliable single-layer out-of-plane micromachined thermal actuator *Sensors Actuators A* **103** 48–58
- [10] Huang Q and Lee N 1999 Analysis and design of polysilicon thermal flexure actuator *J. Micromech. Microeng.* **9** 64–70
- [11] Hickey R, Kujath M and Hubbard T 2002 Heat transfer analysis and optimization of two-beam microelectromechanical thermal actuators *J. Vac. Sci. Technol. A* **20** 971–4
- [12] Li L and Uttamchandani D 2004 Modified asymmetric micro-electrothermal actuator: analysis and experimentation *J. Micromech. Microeng.* **14** 1734–41
- [13] Okada Y and Tokumaru Y 1984 Precise determination of lattice parameter and thermal expansion coefficient of silicon between 300 and 1500 K *J. Appl. Phys.* **15** 314–20